



Article

Fractional Dynamics: Applications of the Caputo Operator in Solving the Sawada–Kotera and Rosenau–Hyman Equations

Khudhayr A. Rashedi ¹, Musawa Yahya Almusawa ^{2,*} , Hassan Almusawa ² , Tariq S. Alshammari ¹ and Adel Almarashi ²

¹ Department of Mathematics, College of Science, University of Ha'il, Ha'il 2440, Saudi Arabia; k.rashedi@uoh.edu.sa (K.A.R.); tas.alshammari@uoh.edu.sa (T.S.A.)

² Department of Mathematics, Faculty of Science, Jazan University, P.O. Box 2097, Jazan 45142, Saudi Arabia; haalmusawa@jazanu.edu.sa (H.A.); aalmarashi@jazanu.edu.sa (A.A.)

* Correspondence: malmusawi@jazanu.edu.sa

Abstract: This study investigates the fractional-order Sawada–Kotera and Rosenau–Hyman equations, which significantly model non-linear wave phenomena in various scientific fields. We employ two advanced methodologies to obtain analytical solutions: the q-homotopy Mohand transform method (q-HMTM) and the Mohand variational iteration method (MVIM). The fractional derivatives in the equations are expressed using the Caputo operator, which provides a flexible framework for analyzing the dynamics of fractional systems. By leveraging these methods, we derive diverse types of solutions, including hyperbolic, trigonometric, and rational forms, illustrating the effectiveness of the techniques in addressing complex fractional models. Numerical simulations and graphical representations are provided to validate the accuracy and applicability of derived solutions. Special attention is given to the influence of the fractional parameter on behavior of the solution behavior, highlighting its role in controlling diffusion and wave propagation. The findings underscore the potential of q-HMTM and MVIM as robust tools for solving non-linear fractional differential equations. They offer insights into their practical implications in fluid dynamics, wave mechanics, and other applications governed by fractional-order models.

Keywords: Sawada–Kotera equation; Rosenau–Hyman equation; q-homotopy Mohand transform method (q-HMTM); Mohand variational iteration method (MVIM); fractional-order differential equation; Caputo operator

MSC: 34G20; 35A20; 35A22; 35R11



Academic Editors: Zhen Chao and Xiang-Sheng Wang

Received: 6 December 2024

Revised: 3 January 2025

Accepted: 7 January 2025

Published: 8 January 2025

Citation: Rashedi, K.A.; Almusawa, M.Y.; Almusawa, H.; Alshammari, T.S.; Almarashi, A. Fractional Dynamics: Applications of the Caputo Operator in Solving the Sawada–Kotera and Rosenau–Hyman Equations. *Mathematics* **2025**, *13*, 193. <https://doi.org/10.3390/math13020193>

Copyright: © 2025 by the authors. Licensee MDPI, Basel, Switzerland. This article is an open access article distributed under the terms and conditions of the Creative Commons Attribution (CC BY) license (<https://creativecommons.org/licenses/by/4.0/>).

1. Introduction

In recent decades, fractional calculus has been demonstrated to have a wide range of applications in a variety of scientific disciplines. Fractional-order derivatives have shown strong agreement with experimental data or real-world phenomena, unlike integer-order derivatives. For example, the non-integer-order derivative more accurately depicts the processing of internal friction, the impact of heredity on the characteristics of various materials, and memory [1–4]. Nowadays, fractional analysis is a crucial tool for describing many phenomena in engineering, physics, chemistry, and other disciplines across one to three dimensions. The attention of researchers is drawn to the latest applications of fractional calculus in many fields, leading to numerous conclusions. Klein–Gordon equations of time fractional order [5,6], fractional diffusion–reaction equation [7], biological population diffusion [8], percolation in porous media [9], fractional model for tuberculosis [10], time

fractional modified anomalous sub-diffusion equation [11], dynamical system [12,13], fractional Drinfeld–Sokolov–Wilson equation [14], fractal vehicular traffic flow [15], fractional KdV Burger–Kuramoto equation [16], space-fractional telegraph equation [17], fractional Buck master’s equation and fractional diffusion [18,19], all benefit from fractional calculus. These discoveries have several scientific applications, including the development of the optimal lighting control approach based on the multi-variable fractional-order extremum searching method [20–22]. Fractional partial differential equations (FPDEs) are the main mathematical framework for explaining various physical processes in applied scientific fields, including engineering, physics, and social sciences [23,24]. Numerous scientific and technical fields, such as biology, fluid dynamics, chemistry, chemical kinetics and physics, use modeling in the form of FPDEs systems [25–30].

The time-fractional generalized fifth-order Sawada–Kotera equation and the time/fractional-order Rosenau–Hyman equation are the subjects of this work. Thus, the application of the Mohand variational iteration technique (MVIM) and the q-homotopy Mohand transform method (q-HMTM) to the problem of the time-fractional Sawada–Kotera equation and the Rosenau–Hyman equation is the primary topic of this study. The exact solutions are then contrasted with the numerical approximations produced by this approach.

Examine the following Sawada–Kotera equation of the time fractional order [31]:

$$D_{\omega}^{\eta} \mathcal{U}(\psi, \omega) = -\frac{\partial^5 \mathcal{U}(\psi, \omega)}{\partial \psi^5} - 15\mathcal{U}(\psi, \omega) \frac{\partial^3 \mathcal{U}(\psi, \omega)}{\partial \psi^3} - 15 \frac{\partial \mathcal{U}(\psi, \omega)}{\partial \psi} \frac{\partial^2 \mathcal{U}(\psi, \omega)}{\partial \psi^2} - 45\mathcal{U}^2(\psi, \omega) \frac{\partial \mathcal{U}(\psi, \omega)}{\partial \psi}, \quad (1)$$

where $0 < \eta \leq 1$.

This is the Sawada–Kotera equation variant of the fifth order [32–35]. The parameter that describes the derivative of the time fractional order in this case is $0 < \eta \leq 1$. In the Caputo sense, the fractional derivative is taken into consideration. The D_{ω}^{η} denotes the Caputo time fractional derivative, and \mathcal{U}_{ψ} represents ordinary integer-order derivative of $\mathcal{U}(\psi, \omega)$ and time is represented by ω .

With several applications in quantum physics and non-linear optics, the classical Sawada–Kotera equation is a significant mathematical model that describes the behavior of long waves in shallow water under gravity and in a one-dimensional non-linear lattice. It is commonly known that bell-shaped sech solutions or kink-shaped tanh solutions may be used to represent fluid dynamics and wave phenomena in plasma media. Waves propagating in opposing directions are also modeled using this equation.

One specific instance of the Gilson–Pickering equation is the Rosenau–Hyman equation. Gilson and Pickering introduced the Gilson–Pickering equation in 1995. The Rosenau–Hyman equation of the time fractional order, which has the following form, is also considered in this study:

$$D_{\omega}^{\eta} \mathcal{U}(\psi, \omega) - \mathcal{U}(\psi, \omega) \frac{\partial^3 \mathcal{U}(\psi, \omega)}{\partial \psi^3} - 3 \frac{\partial \mathcal{U}(\psi, \omega)}{\partial \psi} \frac{\partial^2 \mathcal{U}(\psi, \omega)}{\partial \psi^2} - \mathcal{U}(\psi, \omega) \frac{\partial \mathcal{U}(\psi, \omega)}{\partial \psi} = 0, \quad (2)$$

where $0 < \eta \leq 1$.

The equation was named after Philip Rosenau and James M. Hyman, who conducted the 1993 compactons’ experiment. The Rosenau–Hyman equation provides a simplified model for examining non-linear dispersion in pattern formation in liquid droplets. Additionally, it can represent a wide range of engineering and physics problems [36]. The study of compactons using the Rosenau–Hyman equation is particularly valuable in mathematical physics and applied sciences [37–40]. These applications encourage solving the equation to explore its attributes further. Various methods, such as the reduced differential transform approach [41], the homotopy perturbation method [42], the residual

power series method, the perturbation-iteration algorithm [43], the Genocchi wavelets method [44], and the Laplace-Homotopy Analysis Method [45], have been applied to analyze the Rosenau–Hyman equation.

This paper solves the Sawada–Kotera and Rosenau–Hyman equations using the variational iteration strategy and the q-Homotopy method with a novel transform called the Mohand transform. The variational iteration approach [46–52] has been effectively applied to ODEs [51–63], non-linear polycrystalline solids, and various other disciplines [53–55]. An approximate solution to weakly non-linear systems with one degree of freedom is obtained by combining the perturbation approach, variational iteration method, variation of constants method, and averaging techniques.

Liao introduced the homotopy analysis technique (HAM) [64]. An endless mapping from the starting assumption to a precise response is produced after selecting an auxiliary linear operator. The auxiliary parameter confirms that the solution has converged. When $n \geq 1$ and $q \in [0, 1/n]$, the q-HAM is actually better than $q \in [0, 1]$ in HAM. Adding the parameter $(1/n)^m$ causes the solution to converge faster than the traditional HAM [65–68]. Using semi-analytical approaches with a suitable transform reduces the time required to search for answers for non-linear problems reflecting real-world applications. The q-homotopy Mohand transform method (q-HMTM) combines the Mohand transformation with the q-HAM. What sets it apart is its ability to adapt two strong computational strategies for FDE problems. By choosing the right \hbar , we may control the convergence area of solution series across a large acceptable domain.

This study examines the use of the Mohand variational iteration technique (MVIM) and the q-homotopy Mohand transform method (q-HMTM) to the solution of the fractional-order Sawada–Kotera and Rosenau–Hyman equations. The Caputo operator defines the fractional derivatives. The effectiveness of the proposed approach is demonstrated through solutions to the given problems. Tables and figures illustrate and examine the solutions of the proposed methods. Existing techniques are used to compare findings from time-fractional equations with those from integral-order equations. The proposed method is highly effective for a variety of fractional-order PDEs.

The following is an outline of the rest of this paper: Section 2 explains the Mohand transform basic ideas, the Methodology of the proposed methods is outlined in Section 3, Sections 4 and 5 provides the implementation of the methods, and Conclusions are detailed in Section 6.

2. Mohand Transform Basic Ideas

In this part, we will start by giving a general introduction to the Mohand transform (MT) and associated concepts.

Definition 1. According to [69], the MT is defined for the function $\mathcal{U}(\omega)$ as follows:

$$M[\mathcal{U}(\omega)] = R(s) = s^2 \int_0^\omega \mathcal{U}(\omega) e^{-s\omega} d\omega, \quad k_1 \leq s \leq k_2.$$

An expression of the Mohand inverse transform (MIT) is provided below:

$$M^{-1}[R(s)] = \mathcal{U}(\omega),$$

Definition 2 ([70]). The MT fractional-order derivative is defined as follows:

$$M[\mathcal{U}^\eta(\omega)] = s^\eta R(s) - \sum_{k=0}^{n-1} \frac{\mathcal{U}^k(0)}{s^{k-(\eta+1)}}, \quad 0 < \eta \leq n$$

Definition 3. The following are a few of the MT's characteristics:

1. $M[\mathcal{U}'(\omega)] = sR(s) - s^2R(0),$
2. $M[\mathcal{U}''(\omega)] = s^2R(s) - s^3R(0) - s^2R'(0),$
3. $M[\mathcal{U}^n(\omega)] = s^nR(s) - s^{n+1}R(0) - s^nR'(0) - \dots - s^nR^{n-1}(0).$

Lemma 1. Suppose $\mathcal{U}(\psi, \omega)$ be a function with an exponential order. Then, $M[R(s)] = \mathcal{U}(\psi, \omega)$ describes the MT as follows:

$$M[D_{\omega}^{r\eta}\mathcal{U}(\psi, \omega)] = s^{r\eta}R(s) - \sum_{j=0}^{r-1} s^{\eta(r-j)-1} D_{\omega}^{j\eta}\mathcal{U}(\psi, 0), 0 < \eta \leq 1, \quad (3)$$

where $\psi = (\psi_1, \psi_2, \dots, \psi_{\eta}) \in \mathbb{R}^{\eta}$ and $\eta \in \mathbb{N}$ and $D_{\omega}^{r\eta} = D_{\omega}^{\eta} \cdot D_{\omega}^{\eta} \cdot \dots \cdot D_{\omega}^{\eta}$ (r - times)

Proof. To prove the validity of Equation (1), we will employ the induction technique. To obtain the required result, $r = 1$ may be used to solve Equation (1).

$$M[D_{\omega}^{2\eta}\mathcal{U}(\psi, \omega)] = s^{2\eta}R(s) - s^{2\eta-1}\mathcal{U}(\psi, 0) - s^{\eta-1}D_{\omega}^{\eta}\mathcal{U}(\psi, 0).$$

The validity of Equation (1) for $r = 1$ is demonstrated by Definition 2. Solve Equation (1) by inserting $r = 2$.

$$M[D_r^{2\eta}\mathcal{U}(\psi, \omega)] = s^{2\eta}R(s) - s^{2\eta-1}\mathcal{U}(\psi, 0) - s^{\eta-1}D_{\omega}^{\eta}\mathcal{U}(\psi, 0). \quad (4)$$

Consider the left-hand side of Equation (4):

$$L.H.S = M[D_{\omega}^{2\eta}\mathcal{U}(\psi, \omega)]. \quad (5)$$

Equation (5) is also represented as

$$L.H.S = M[D_{\omega}^{\eta}D_{\omega}^{\eta}\mathcal{U}(\psi, \omega)]. \quad (6)$$

Assume

$$z(\psi, \omega) = D_{\omega}^{\eta}\mathcal{U}(\psi, \omega). \quad (7)$$

Equation (7) should be substituted in Equation (6):

$$L.H.S = M[D_{\omega}^{\eta}z(\psi, \omega)]. \quad (8)$$

The Caputo derivative results in the following modifications being made to Equation (8):

$$L.H.S = M[J^{1-\eta}z'(\psi, \omega)]. \quad (9)$$

The following modification to Equation (9) is brought about by the RL integral:

$$L.H.S = \frac{M[z'(\psi, \omega)]}{s^{1-\eta}}. \quad (10)$$

These results are derived from Equation (61) by means of the MT derivative characteristic.

$$L.H.S = s^{\eta}Z(\psi, s) - \frac{z(\psi, 0)}{s^{1-\eta}}, \quad (11)$$

This result was obtained using Equation (7).

$$Z(\psi, s) = s^\eta R(s) - \frac{\mathcal{U}(\psi, 0)}{s^{1-\eta}},$$

As $M[z(\omega, \psi)] = Z(\psi, s)$. Thus, Equation (11) is also represented as

$$L.H.S = s^{2\eta} R(s) - \frac{\mathcal{U}(\psi, 0)}{s^{1-2\eta}} - \frac{D_\omega^\eta \mathcal{U}(\psi, 0)}{s^{1-\eta}}, \quad (12)$$

Assume that for $r = K$, Equation (1) is true. In Equation (1), put $r = K$.

$$M[D_\omega^{K\eta} \mathcal{U}(\psi, \omega)] = s^{K\eta} R(s) - \sum_{j=0}^{K-1} s^{\eta(K-j)-1} D_\omega^{j\eta} D_\omega^{j\eta} \mathcal{U}(\psi, 0), \quad 0 < \eta \leq 1. \quad (13)$$

Further, we have to prove that Equation (1) is valid for $r = K + 1$. To solve Equation (1), put $r = K + 1$.

$$M[D_\omega^{(K+1)\eta} \mathcal{U}(\psi, \omega)] = s^{(K+1)\eta} R(s) - \sum_{j=0}^K s^{\eta((K+1)-j)-1} D_\omega^{j\eta} \mathcal{U}(\psi, 0). \quad (14)$$

This result is derived from Equation (14).

$$L.H.S = M[D_\omega^{K\eta} (D_\omega^{K\eta})]. \quad (15)$$

Let

$$D_\omega^{K\eta} = g(\psi, \omega).$$

By employing Equation (15), the subsequent result is achieved:

$$L.H.S = M[D_\omega^\eta g(\psi, \omega)]. \quad (16)$$

Equation (16) is modified by employing Caputo's derivative and the RL integral.

$$L.H.S = s^\eta M[D_\omega^{K\eta} \mathcal{U}(\psi, \omega)] - \frac{g(\psi, 0)}{s^{1-\eta}}. \quad (17)$$

Equation (63) can serve as a basis for the formulation of Equation (17).

$$L.H.S = s^{r\eta} R(s) - \sum_{j=0}^{r-1} s^{\eta(r-j)-1} D_\omega^{j\eta} \mathcal{U}(\psi, 0), \quad (18)$$

An alternate form of Equation (18) is

$$L.H.S = M[D_\omega^{r\eta} \mathcal{U}(\psi, 0)].$$

Equation (1) is proven to hold for $r = K + 1$ using mathematical induction. For all positive integers, it has been proved that Equation (1) is true. \square

Lemma 2. Let $\mathcal{U}(\psi, \omega)$ be an exponentially ordered function. $M[\mathcal{U}(\psi, \omega)] = R(s)$ denotes the MT of $\mathcal{U}(\psi, \omega)$. The multiple fractional power series (MFPS) is shown as follows in relation to the Mohand transform:

$$R(s) = \sum_{r=0}^{\infty} \frac{\hbar_r(\psi)}{s^{r\eta+1}}, \quad s > 0, \quad (19)$$

where $\psi = (s_1, \psi_2, \dots, \psi_\eta) \in \mathbb{R}^\eta$, $\eta \in \mathbb{N}$.

Proof. Assume the Taylor series:

$$\mathcal{U}(\psi, \omega) = \hbar_0(\psi) + \hbar_1(\psi) \frac{\omega^\eta}{\Gamma[\eta + 1]} + \hbar_2(\psi) \frac{\omega^{2\eta}}{\Gamma[2\eta + 1]} + \dots \quad (20)$$

Equation (20) yields the following result when MT is applied:

$$M[\mathcal{U}(\psi, \omega)] = M[\hbar_0(\psi)] + M\left[\hbar_1(\psi) \frac{\omega^\eta}{\Gamma[\eta + 1]}\right] + M\left[\hbar_2(\psi) \frac{\omega^{2\eta}}{\Gamma[2\eta + 1]}\right] + \dots$$

Use MT's characteristics to accomplish this result.

$$M[\mathcal{U}(\psi, \omega)] = \hbar_0(\psi) \frac{1}{s} + \hbar_1(\psi) \frac{\Gamma[\eta + 1]}{\Gamma[\eta + 1]} \frac{1}{s^{\eta+1}} + \hbar_2(\psi) \frac{\Gamma[2\eta + 1]}{\Gamma[2\eta + 1]} \frac{1}{s^{2\eta+1}} \dots$$

As a result, the Taylor series in an improved form is obtained. \square

Lemma 3. The improved Taylor series in MFPS is as follows, assuming that $M[\mathcal{U}(\psi, \omega)] = R(s)$ denotes MT:

$$\hbar_0(\psi) = \lim_{s \rightarrow \infty} sR(s) = \mathcal{U}(\psi, 0). \quad (21)$$

Proof. Assume the Taylor series:

$$\hbar_0(\psi) = sR(s) - \frac{\hbar_1(\psi)}{s^\eta} - \frac{\hbar_2(\psi)}{s^{2\eta}} - \dots \quad (22)$$

Calculate and simplify the limit given in Equation (21) to obtain Equation (22). \square

Theorem 1. Let $M[\mathcal{U}(\psi, \omega)]$ be a function. In the MFPS form, $R(s)$ is represented as follows:

$$R(s) = \sum_{r=0}^{\infty} \frac{\hbar_r(\psi)}{s^{r\eta+1}}, \quad s > 0,$$

where $\psi = (\psi_1, \psi_2, \dots, \psi_\eta) \in \mathbb{R}^\eta$ and $\eta \in \mathbb{N}$. Then, we have

$$\hbar_r(\psi) = D_r^{\eta} \mathcal{U}(\psi, 0),$$

where $D_\omega^{r\eta} = D_\omega^\eta \cdot D_\omega^\eta \cdot \dots \cdot D_\omega^\eta$ (r - times).

Proof. Assume the Taylor series:

$$\hbar_1(\psi) = s^{\eta+1}R(s) - s^\eta \hbar_0(\psi) - \frac{\hbar_2(\psi)}{s^\eta} - \frac{\hbar_3(\psi)}{s^{2\eta}} - \dots \quad (23)$$

The following result is obtained by applying the limit to Equation (23):

$$\hbar_1(\psi) = \lim_{s \rightarrow \infty} (s^{\eta+1}R(s) - s^\eta \hbar_0(\psi)) - \lim_{s \rightarrow \infty} \frac{\hbar_2(\psi)}{s^\eta} - \lim_{s \rightarrow \infty} \frac{\hbar_3(\psi)}{s^{2\eta}} - \dots$$

We obtain the subsequent result after simplification:

$$\hbar_1(\psi) = \lim_{s \rightarrow \infty} (s^{\eta+1}R(s) - s^\eta \hbar_0(\psi)). \quad (24)$$

Lemma 1 introduces the fundamental concepts that are employed to derive the following form of Equation (24):

$$\hbar_1(\psi) = \lim_{s \rightarrow \infty} (sM[D_\omega^\eta \mathcal{U}(\psi, \omega)](s)). \quad (25)$$

The following is the formulation of Equation (25) that uses Lemma 2 as a basis:

$$\hbar_1(\psi) = D_{\omega}^{\eta} \mathcal{U}(\psi, 0).$$

To obtain the subsequent result, it is necessary to take $\lim_{s \rightarrow \infty}$ once more and apply the Taylor series.

$$\hbar_2(\psi) = s^{2\eta+1} R(s) - s^{2\eta} \hbar_0(\psi) - s^{\eta} \hbar_1(\psi) - \frac{\hbar_3(\psi)}{s^{\eta}} - \dots$$

Applying Lemma 2 yields the subsequent results:

$$\hbar_2(\psi) = \lim_{s \rightarrow \infty} s(s^{2\eta} R(s) - s^{2\eta-1} \hbar_0(\psi) - s^{\eta-1} \hbar_1(\psi)). \quad (26)$$

By employing Lemmas 1 and 3 as a base, Equation (26) can be modified in the following manner:

$$\hbar_2(\psi) = D_{\omega}^{2\eta} \mathcal{U}(\psi, 0).$$

By employing the same procedure, we obtain

$$\hbar_3(\psi) = \lim_{s \rightarrow \infty} s(M[D_{\omega}^{2\eta} \mathcal{U}(\psi, \eta)](s)).$$

In order to achieve this ultimate result, Lemma 3 is implemented.

$$\hbar_3(\psi) = D_{\omega}^{3\eta} \mathcal{U}(\psi, 0).$$

Generally,

$$\hbar_r(\psi) = D_{\omega}^{r\eta} \mathcal{U}(\psi, 0).$$

□

In the subsequent theorem, the improved form of Taylor's series convergence is explicated and illustrated.

Theorem 2. In accordance with the application of Lemma 2, the MFTS expression is provided as follows: $M[\mathcal{U}(\omega, \psi)] = R(s)$. When $|s^a M[D_{\omega}^{(K+1)\eta} \mathcal{U}(\psi, \omega)]| \leq T$, for all $s > 0$ and $0 < \eta \leq 1$, the residual $H_K(\psi, s)$ of the MFTS and validate the inequality:

$$|H_K(\psi, s)| \leq \frac{T}{s^{(K+1)\eta+1}}, \quad s > 0.$$

Proof. Let $M[D_{\omega}^{r\eta} \mathcal{U}(\psi, \omega)](s)$ is defined on $s > 0$ for $r = 0, 1, 2, \dots, K+1$ and consider $|sM[D_{\omega}^{K+1} \mathcal{U}(\psi, \omega)]| \leq T$. The resultant relationship may be determined by applying the revised Taylor series.

$$H_K(\psi, s) = R(s) - \sum_{r=0}^K \frac{\hbar_r(\psi)}{s^{r\eta+1}}. \quad (27)$$

The following result can be achieved by employing Equation (27) and Theorem 1:

$$H_K(\psi, s) = R(s) - \sum_{r=0}^K \frac{D_{\omega}^{r\eta} \mathcal{U}(\psi, 0)}{s^{r\eta+1}}. \quad (28)$$

Multiply Equation (28) by $s^{(K+1)\eta+1}$:

$$s^{(K+1)\eta+1} H_K(\psi, s) = s(s^{(K+1)\eta} R(s) - \sum_{r=0}^K s^{(K+1-r)\eta-1} D_{\omega}^{r\eta} \mathcal{U}(\psi, 0)). \quad (29)$$

The application of Lemma 1 results in the following form of Equation (29):

$$s^{(K+1)\eta+1}H_K(\psi, s) = sM[D_\omega^{(K+1)\eta}\mathcal{U}(\psi, \omega)]. \quad (30)$$

Take the absolute

$$|s^{(K+1)\eta+1}H_K(\psi, s)| = |sM[D_\omega^{(K+1)\eta}\mathcal{U}(\psi, \omega)]|. \quad (31)$$

The condition of Equation (31) must be implemented in order to achieve the desired result.

$$\frac{-T}{s^{(K+1)\eta+1}} \leq H_K(\psi, s) \leq \frac{T}{s^{(K+1)\eta+1}}. \quad (32)$$

The subsequent result is obtained from Equation (32).

$$|H_K(\psi, s)| \leq \frac{T}{s^{(K+1)\eta+1}}.$$

This leads to the development of a new criteria for the convergence of the series. \square

3. Methodology

3.1. q -Homotopy Mohand Transform Method (q -HMTM)

Let us examine a PDE of a time fractional order that is non-homogeneous and non-linear:

$$D_\omega^\eta \mathcal{U}(\psi, \omega) + \mathcal{R}\mathcal{U}(\psi, \omega) + \mathcal{N}\mathcal{U}(\psi, \omega) = \mathbb{H}(\psi, \omega), \quad n-1 < \eta \leq n. \quad (33)$$

The non-linear and linear operators are denoted by \mathcal{N} and \mathcal{R} , respectively, while the Caputo derivative is denoted by $D_\omega^\eta \mathcal{U}(\psi, \omega)$. $\mathbb{H}(\psi, \omega)$ is the source term.

Apply the transformation of Mohand transformation on Equation (33).

$$\mathcal{M}[\mathcal{U}(\psi, \omega)] - \frac{1}{s^\eta} \sum_{k=0}^{n-1} s^{\eta-k-1} \mathcal{U}^k(\psi, 0) + \frac{1}{s^\eta} [\mathcal{M}[\mathcal{R}\mathcal{U}(\psi, \omega)] + \mathcal{M}[\mathcal{N}\mathcal{U}(\psi, \omega)] - \mathcal{M}[\mathbb{H}(\psi, \omega)]] = 0, \quad (34)$$

The non-linear operator is defined as follows:

$$\begin{aligned} N[\varphi(\psi, \omega; q)] &= \mathcal{M}[\varphi(\psi, \omega; q)] - \frac{1}{s^\eta} \sum_{k=0}^{n-1} s^{\eta-k-1} \varphi^k(\psi, \omega; q)(0^+) + \frac{1}{s^\eta} [\mathcal{M}[\mathcal{R}\varphi(\psi, \omega; q)] \\ &+ \mathcal{M}[\mathcal{N}\varphi(\psi, \omega; q)] - \mathcal{M}[\mathbb{H}(\psi, \omega)]], \end{aligned} \quad (35)$$

In the present case, $\varphi(\psi, \omega; q)$ with respect to ψ , ω , and $q \in \left[0, \frac{1}{n}\right]$ is a real-valued function. A homotopy can be defined as

$$(1 - nq)\mathcal{M}[\varphi(\psi, \omega; q) - \mathcal{U}_0(\psi, \omega)] = \hbar q \mathbb{H}(\psi, \omega) \mathcal{N}[\varphi(\psi, \omega; q)], \quad (36)$$

where the auxiliary parameter is $\hbar \neq 0$ and the initial condition is \mathcal{U}_0 .

The succeeding result is valid for 0 and $\frac{1}{n}$.

$$\varphi(\psi, \omega; 0) = \mathcal{U}_0(\psi, \omega), \quad \varphi(\psi, \omega; \frac{1}{n}) = \mathcal{U}(\psi, \omega), \quad (37)$$

As a consequence of the intensification of q , the solution $\varphi(\psi, \omega; q)$ differs from the initial condition $\mathcal{U}_0(\psi, \omega)$ to $\mathcal{U}(\psi, \omega)$. By employing the Taylor theorem to define $\varphi(\psi, \omega; q)$ in relation to q , we can derive the following:

$$\varphi(\psi, \omega; q) = \mathcal{U}_0(\psi, \omega) + \sum_{m=1}^{\infty} \mathcal{U}_m(\psi, \omega) q^m, \quad (38)$$

where

$$\mathcal{U}_m = \frac{1}{m!} \frac{\partial^m \varphi(\psi, \omega; q)}{\partial q^m} \Big|_{q=0}, \quad (39)$$

The series (36) converges at $q = \frac{1}{n}$ for the appropriate values of $\mathcal{U}_0(\psi, \omega)$, n , and \hbar . Subsequently,

$$\varphi(\psi, \omega; q) = \mathcal{U}_0(\psi, \omega) + \sum_{m=1}^{\infty} \mathcal{U}_m(\psi, \omega) \left(\frac{1}{n}\right)^m, \quad (40)$$

By setting $q = 0$, dividing by $m!$, and calculating the derivative of Equation (36) with regard to the embedding parameter q , the following is obtained:

$$\mathcal{M}[\mathcal{U}_m(\psi, \omega) - k_m \mathcal{U}_{m-1}(\psi, \omega)] = \hbar \mathfrak{h}(\psi, \omega) \mathcal{R}_m(\vec{\mathcal{U}}_{m-1}), \quad (41)$$

The vectors and the auxiliary parameter $\hbar \neq 0$ are subsequently defined as

$$\vec{\mathcal{U}}_m = [\mathcal{U}_0(\psi, \omega), \mathcal{U}_1(\psi, \omega), \dots, \mathcal{U}_m(\psi, \omega)], \quad (42)$$

The result of the application of the inverse Mohand transform to Equation (41) is as follows:

$$\mathcal{U}_m(\psi, \omega) = k_m \mathcal{U}_{m-1}(\psi, \omega) + \hbar \mathcal{M}^{-1}[\mathfrak{h}(\psi, \omega) \mathcal{R}_m(\vec{\mathcal{U}}_{m-1})], \quad (43)$$

$$\mathcal{R}_m(\vec{\mathcal{U}}_{m-1}) = \frac{1}{(m-1)!} \frac{\partial^{m-1} \mathcal{N}[\varphi(\psi, \omega; q)]}{\partial q^{m-1}} \Big|_{q=0},$$

$$k_m = \begin{cases} 0 & \text{if } m \leq 1, \\ 1 & \text{if } m > 1, \end{cases} \quad (44)$$

Finally, the components of the q-HMTM solution are determined by solving Equation (43).

3.2. Mohand Variation Iteration Transform Method (MVIM)

Let us examine a PDE of a time fractional order that is non-homogeneous and non-linear:

$$D_{\omega}^{\eta} \mathcal{U}(\psi, \omega) = \mathcal{R}\mathcal{U}(\psi, \omega) + \mathcal{N}\mathcal{U}(\psi, \omega) + \mathbb{H}(\psi, \omega), \quad n-1 < \eta \leq n. \quad (45)$$

Initial condition

$$\mathcal{U}(\psi, 0) = \mathcal{U}_0(\psi). \quad (46)$$

Take MT of Equation (45).

$$\mathcal{M}[D_{\omega}^{\eta} \mathcal{U}(\psi, \omega)] = \mathcal{M}[\mathcal{R}\mathcal{U}(\psi, \omega) + \mathcal{N}\mathcal{U}(\psi, \omega) + \mathbb{H}(\psi, \omega)], \quad (47)$$

The following can be accomplished by utilizing the iteration property of transform:

$$\mathcal{M}[\mathcal{U}(\psi, \omega)] - \sum_{k=0}^{m-1} s^{\eta-k-1} \frac{\partial^k \mathcal{U}(\psi, \omega)}{\partial \omega^k} \Big|_{\omega=0} = \mathcal{M}[\mathcal{R}\mathcal{U}(\psi, \omega) + \mathcal{N}\mathcal{U}(\psi, \omega) + \mathbb{H}(\psi, \omega)], \quad (48)$$

by employing an iterative process that integrates the Lagrange multiplier $(-\lambda(s))$,

$$\mathcal{M}[\mathcal{U}_{n+1}(\psi, \omega)] = \mathcal{M}[\mathcal{U}_n(\psi, \omega)] - \lambda(s) \left[\mathcal{M}[\mathcal{U}_n(\psi, \omega)] - \sum_{k=0}^{m-1} s^{\eta-k-1} \frac{\partial^k \mathcal{U}(\psi, 0)}{\partial \omega^k} \right], \quad (49)$$

Substitute Equation (49) into Equation (48) and take $\lambda(s) = -\frac{1}{s^\eta}$.

$$\begin{aligned} \mathcal{M}[\mathcal{U}_{n+1}(\psi, \omega)] &= \mathcal{M}[\mathcal{U}_n(\psi, \omega)] - \lambda(s) \left[\mathcal{M}[\mathcal{U}_n(\psi, \omega)] - \sum_{k=0}^{m-1} s^{\eta-k-1} \frac{\partial^k \mathcal{U}(\psi, 0)}{\partial \omega^k} \right. \\ &\quad \left. + \mathcal{M}[\mathcal{R}\mathcal{U}(\psi, \omega) + \mathcal{N}\mathcal{U}(\psi, \omega) + \mathbb{H}(\psi, \omega)] \right], \end{aligned} \quad (50)$$

Apply MIT on Equation (50).

$$\begin{aligned} \mathcal{U}_{n+1}(\psi, \omega) &= \mathcal{U}_n(\psi, \omega) + \mathcal{M}^{-1} \left[\frac{1}{s^\eta} \sum_{k=0}^{m-1} s^{\eta-k-1} \frac{\partial^k \mathcal{U}(\psi, 0)}{\partial \omega^k} \right. \\ &\quad \left. + \mathcal{M}[\mathcal{R}\mathcal{U}(\psi, \omega) + \mathcal{N}\mathcal{U}(\psi, \omega) + \mathbb{H}(\psi, \omega)] \right], \end{aligned} \quad (51)$$

The initial condition is given as

$$\mathcal{U}_0(\psi, \omega) = \mathcal{M}^{-1} \left[\frac{1}{s^\eta} \sum_{k=0}^{m-1} s^{\eta-k-1} \frac{\partial^k \mathcal{U}(\psi, 0)}{\partial \omega^k} \right], \quad (52)$$

The recursive scheme is described as follows:

$$\begin{aligned} \mathcal{U}_{n+1}(\psi, \omega) &= \mathcal{U}_n(\psi, \omega) + \mathcal{M}^{-1} \left[\frac{1}{s^\eta} \sum_{k=0}^{m-1} s^{\eta-k-1} \frac{\partial^k \mathcal{U}(\psi, 0)}{\partial \omega^k} \right. \\ &\quad \left. + \mathcal{M}[\mathcal{R}\mathcal{U}(\psi, \omega) + \mathcal{N}\mathcal{U}(\psi, \omega) + \mathbb{H}(\psi, \omega)] \right], \end{aligned} \quad (53)$$

4. Problem 1

4.1. Solution via q -Homotopy Mohand Transform Method

Consider the time fractional-order Sawada–Kotera equation:

$$D_\omega^\eta \mathcal{U}(\psi, \omega) + \frac{\partial^5 \mathcal{U}(\psi, \omega)}{\partial \psi^5} + 15\mathcal{U}(\psi, \omega) \frac{\partial^3 \mathcal{U}(\psi, \omega)}{\partial \psi^3} + 15 \frac{\partial \mathcal{U}(\psi, \omega)}{\partial \psi} \frac{\partial^2 \mathcal{U}(\psi, \omega)}{\partial \psi^2} + 45\mathcal{U}^2(\psi, \omega) \frac{\partial \mathcal{U}(\psi, \omega)}{\partial \psi} = 0, \quad (54)$$

where $0 < \eta \leq 1$.

ICs are given as

$$\mathcal{U}(\psi, 0) = 2k^2 \text{sech}^2(k\psi), \quad (55)$$

$$\begin{aligned} \mathcal{M}[\mathcal{U}(\psi, \omega)] + s \left(2k^2 \text{sech}^2(k\psi) \right) + \frac{1}{s^\eta} \mathcal{M} \left[\frac{\partial^5 \mathcal{U}(\psi, \omega)}{\partial \psi^5} + 15\mathcal{U}(\psi, \omega) \frac{\partial^3 \mathcal{U}(\psi, \omega)}{\partial \psi^3} + 15 \frac{\partial \mathcal{U}(\psi, \omega)}{\partial \psi} \frac{\partial^2 \mathcal{U}(\psi, \omega)}{\partial \psi^2} \right. \\ \left. + 45\mathcal{U}^2(\psi, \omega) \frac{\partial \mathcal{U}(\psi, \omega)}{\partial \psi} \right] = 0. \end{aligned} \quad (56)$$

The non-linear operators are define as

$$\begin{aligned} \mathcal{N}[\varphi(\psi, \omega; q)] &= \mathcal{M}[\varphi(\psi, \omega; q)] + s \left(2k^2 \text{sech}^2(k\psi) \right) + \frac{1}{s^\eta} \mathcal{M} \left[\frac{\partial^5 \varphi(\psi, \omega; q)}{\partial \psi^5} + 15\varphi(\psi, \omega; q) \frac{\partial^3 \varphi(\psi, \omega; q)}{\partial \psi^3} \right. \\ &\quad \left. + 15 \frac{\partial \varphi(\psi, \omega; q)}{\partial \psi} \frac{\partial^2 \varphi(\psi, \omega; q)}{\partial \psi^2} + 45\varphi^2(\psi, \omega; q) \frac{\partial \varphi(\psi, \omega; q)}{\partial \psi} \right], \end{aligned} \quad (57)$$

and the Mohand operators are define as

$$\mathcal{M}[\mathcal{U}_m(\psi, \omega) - k_m \mathcal{U}_{m-1}(\psi, \omega)] = \hbar \mathfrak{h}(\psi, \omega) \mathcal{R}_m[\rightarrow U_{m-1}]. \quad (58)$$

Here,

$$\begin{aligned} \mathcal{R}_m[\rightarrow U_{m-1}] = & \mathcal{M}[\mathcal{U}_{m-1}(\psi, \omega)] + \left(1 - \frac{k_m}{n}\right) s \left(2k^2 \operatorname{sech}^2(k\psi)\right) + \frac{1}{s^\eta} \mathcal{M} \left[\frac{\partial^5 \mathcal{U}_{m-1}(\psi, \omega)}{\partial \psi^5} \right. \\ & + 15 \sum_{i=0}^{m-1} \mathcal{U}_i(\psi, \omega) \frac{\partial^3 \mathcal{U}_{m-1-i}(\psi, \omega)}{\partial \psi^3} + 15 \sum_{i=0}^{m-1} \frac{\partial \mathcal{U}_i(\psi, \omega)}{\partial \psi} \frac{\partial^2 \mathcal{U}_{m-1-i}(\psi, \omega)}{\partial \psi^2} + 45 \sum_{r=0}^{m-1} \sum_{i=0}^{m-1-r} \mathcal{U}(\psi, \omega)_r \mathcal{U}(\psi, \omega)_i \times \\ & \left. \frac{\partial \mathcal{U}_{m-1-r-i}(\psi, \omega)}{\partial \psi} \right], \end{aligned} \quad (59)$$

$$\mathcal{U}_m(\psi, \omega) = k_m \mathcal{U}_{m-1}(\psi, \omega) + \hbar \mathcal{M}^{-1}[\mathfrak{h}(\psi, \omega) \mathcal{R}_m(\rightarrow U_{m-1})]. \quad (60)$$

Based on the initial constraint of Equation (60), the subsequent result is obtained:

$$\begin{aligned} \mathcal{U}_1(\psi, \omega) &= -\frac{64k^7 \hbar \omega^\eta \tanh(\psi k) \operatorname{sech}^2(k\psi)}{\Gamma(\eta + 1)}, \\ \mathcal{U}_2(\psi, \omega) &= 32k^7 \hbar \omega^\eta \operatorname{sech}^4(k\psi) \left(\frac{32k^5 \hbar \omega^\eta (\cosh(2k\psi) - 2)}{\Gamma(2\eta + 1)} - \frac{(n + \hbar) \sinh(2k\psi)}{\Gamma(\eta + 1)} \right). \end{aligned} \quad (61)$$

and so on.

In the same way, the remaining components are acquired. The q-HMTM solution of Equation (54) is subsequently derived.

$$\mathcal{U}(\psi, \omega) = \mathcal{U}_0 + \sum_{m=1}^{\infty} \mathcal{U}_m \left(\frac{1}{n} \right)^m. \quad (62)$$

$$\begin{aligned} \mathcal{U}(\psi, \omega) = & 2k^2 \operatorname{sech}^2(k\psi) - \frac{64k^7 \hbar \omega^\eta \tanh(k\psi) \operatorname{sech}^2(k\psi)}{\Gamma(\eta + 1)} + 32k^7 \hbar \omega^\eta \operatorname{sech}^4(k\psi) \left(\frac{32k^5 \hbar \omega^\eta (\cosh(2k\psi) - 2)}{\Gamma(2\eta + 1)} \right. \\ & \left. - \frac{(n + \hbar) \sinh(2k\psi)}{\Gamma(\eta + 1)} \right) + \dots \end{aligned} \quad (63)$$

The approximate solution $\sum_{m=1}^N \mathcal{U}_m \left(\frac{1}{n} \right)^m$ for the values $\eta = 1$, $\hbar = -1$ and $n = 1$ converges to the exact solution as $N \rightarrow \infty$.

$$\mathcal{U}(\psi, \omega) = 2k^2 \operatorname{sech}^2(k\psi - 16\omega k^5). \quad (64)$$

4.2. Solution via Mohand Variational Iteration Transform Method

Consider the time fractional-order Sawada–Kotera equation:

$$D_\omega^\eta \mathcal{U}(\psi, \omega) = -\frac{\partial^5 \mathcal{U}(\psi, \omega)}{\partial \psi^5} - 15 \mathcal{U}(\psi, \omega) \frac{\partial^3 \mathcal{U}(\psi, \omega)}{\partial \psi^3} - 15 \frac{\partial \mathcal{U}(\psi, \omega)}{\partial \psi} \frac{\partial^2 \mathcal{U}(\psi, \omega)}{\partial \psi^2} - 45 \mathcal{U}^2(\psi, \omega) \frac{\partial \mathcal{U}(\psi, \omega)}{\partial \psi}, \quad (65)$$

where $0 < \eta \leq 1$.

ICs are given as

$$\mathcal{U}(\psi, 0) = 2k^2 \operatorname{sech}^2(k\psi), \quad (66)$$

The following result is obtained by employing the iterative scheme (53):

$$\begin{aligned} \mathcal{U}_{n+1}(\psi, \omega) = & \mathcal{U}_n(\psi, \omega) + \mathcal{M}^{-1} \left[\frac{1}{s^\eta} \sum_{k=0}^{m-1} s^{\eta-k-1} \frac{\partial^k \mathcal{U}(\psi, 0)}{\partial \omega^k} + \mathcal{M} \left[-\frac{\partial^5 \mathcal{U}_n(\psi, \omega)}{\partial \psi^5} - 15 \mathcal{U}_n(\psi, \omega) \frac{\partial^3 \mathcal{U}_n(\psi, \omega)}{\partial \psi^3} \right. \right. \\ & \left. \left. - 15 \frac{\partial \mathcal{U}_n(\psi, \omega)}{\partial \psi} \frac{\partial^2 \mathcal{U}_n(\psi, \omega)}{\partial \psi^2} - 45 \mathcal{U}_n^2(\psi, \omega) \frac{\partial \mathcal{U}_n(\psi, \omega)}{\partial \psi} \right] \right], \end{aligned} \quad (67)$$

To obtain the second approximate solution, put $n = 0$.

$$\begin{aligned} \mathcal{U}_1(\psi, \omega) = & \mathcal{U}_0(\psi, \omega) + \mathcal{M}^{-1} \left[\frac{1}{s^\eta} \sum_{k=0}^{m-1} s^{\eta-k-1} \frac{\partial^k \mathcal{U}(\psi, 0)}{\partial \omega^k} + \mathcal{M} \left[-\frac{\partial^5 \mathcal{U}_0(\psi, \omega)}{\partial \psi^5} - 15 \mathcal{U}_0(\psi, \omega) \frac{\partial^3 \mathcal{U}_0(\psi, \omega)}{\partial \psi^3} \right. \right. \\ & \left. \left. - 15 \frac{\partial \mathcal{U}_0(\psi, \omega)}{\partial \psi} \frac{\partial^2 \mathcal{U}_0(\psi, \omega)}{\partial \psi^2} - 45 \mathcal{U}_0^2(\psi, \omega) \frac{\partial \mathcal{U}_0(\psi, \omega)}{\partial \psi} \right] \right], \end{aligned} \quad (68)$$

The subsequent result is obtained by simplifying the previous result:

$$\mathcal{U}_1(\psi, \omega) = 2k^2 \operatorname{sech}^2(\psi k) + \frac{64k^7 \omega^\eta \tanh(\psi k) \operatorname{sech}^2(\psi k)}{\Gamma(\eta + 1)}. \quad (69)$$

By inserting $n = 1$, we obtain

$$\begin{aligned} \mathcal{U}_2(\psi, \omega) = & \mathcal{U}_1(\psi, \omega) + \mathcal{M}^{-1} \left[\frac{1}{s^\eta} \sum_{k=0}^{m-1} s^{\eta-k-1} \frac{\partial^k \mathcal{U}(\psi, 0)}{\partial \omega^k} + \mathcal{M} \left[-\frac{\partial^5 \mathcal{U}_1(\psi, \omega)}{\partial \psi^5} - 15 \mathcal{U}_1(\psi, \omega) \frac{\partial^3 \mathcal{U}_1(\psi, \omega)}{\partial \psi^3} \right. \right. \\ & \left. \left. - 15 \frac{\partial \mathcal{U}_1(\psi, \omega)}{\partial \psi} \frac{\partial^2 \mathcal{U}_1(\psi, \omega)}{\partial \psi^2} - 45 \mathcal{U}_1^2(\psi, \omega) \frac{\partial \mathcal{U}_1(\psi, \omega)}{\partial \psi} \right] \right], \end{aligned} \quad (70)$$

The final approximate solution that emerges from the simplification is as follows:

$$\begin{aligned} \mathcal{U}_2(\psi, \omega) = & 2k^2 \operatorname{sech}^2(\psi k) + \frac{64k^7 \omega^\eta \tanh(\psi k) \operatorname{sech}^2(\psi k)}{\Gamma(\eta + 1)} + \frac{1024k^{12} \omega^{2\eta} (\cosh(2\psi k) - 2) \operatorname{sech}^4(\psi k)}{\Gamma(2\eta + 1)} \\ & + \frac{122880k^{17} \omega^{3\eta} \Gamma(2\eta + 1) (-11 \cosh(2\psi k) + \cosh(4\psi k) + 12) \tanh(\psi k) \operatorname{sech}^8(\psi k)}{\Gamma(\eta + 1)^2 \Gamma(3\eta + 1)} \\ & + \frac{11796480k^{22} \omega^{4\eta} \Gamma(3\eta + 1) \cosh(2\psi k) \tanh^2(\psi k) \operatorname{sech}^8(\psi k)}{\Gamma(\eta + 1)^3 \Gamma(4\eta + 1)}. \end{aligned} \quad (71)$$

The time fractional-order Sawada–Kotera equation is thoroughly analyzed by comparing solutions obtained through the MVIM and q-HMTM methods. The results are systematically presented in tables and figures to illustrate the effectiveness and accuracy of the methodologies. Table 1 highlights the comparison of solutions $\mathcal{U}(\psi, \omega)$ derived using MVIM and q-HMTM for different fractional orders η of Equation (65). The table reveals a strong agreement between the two methods, demonstrating their reliability in solving fractional-order models. Figure 1 provides a graphical comparison of the solution $\mathcal{U}(\psi, \omega)$ for varying fractional orders η : Figure 1a: Depicts the effect of $\eta = 0.5$ on the solution, illustrating slower diffusion and wave propagation. Figure 1b: Explores the behavior at $\eta = 0.7$, showing enhanced wave characteristics compared to lower orders. Figure 1c: Represents the case of $\eta = 1.0$, corresponding to the classical integer-order scenario, with distinct waveforms. Figure 1d: Displays a 2D comparison of the solution $\mathcal{U}(\psi, \omega)$ at $\omega = 0.1$, highlighting the consistency between methods. Figure 2 showcases both 3D and 2D representations of the exact and approximate solutions $\mathcal{U}(\psi, \omega)$ for $\omega = 0.1$ of Equation (65). These visualizations emphasize the high degree of accuracy achieved by the approximate methods, with minimal deviations from the exact solution. Table 2 provides a detailed error

analysis for the MVIM and q-HMTM methods when applied to $\mathcal{U}(\psi, \omega)$ across different fractional orders η . The error values are consistently low, confirming the precision and robustness of both techniques. The table also underscores the superiority of q-HMTM in scenarios with higher fractional orders.

Table 1. MVIM and q-HMTM solution comparison of $\mathcal{U}(\psi, \omega)$ for different fractional orders η of Equation (65).

ω	ψ	q-HMTM	MVIM	q-HMTM	MVIM	q-HMTM	MVIM	Exact
		$\eta = 0.5$	$\eta = 0.5$	$\eta = 0.7$	$\eta = 0.7$	$\eta = 1.0$	$\eta = 1.0$	
0.01	0.2	0.498199	0.498362	0.496888	0.496896	0.495515	0.495515	0.495515
	0.6	0.470904	0.471064	0.463191	0.463198	0.458893	0.458893	0.458893
	1.0	0.413022	0.412863	0.401095	0.401087	0.395037	0.395037	0.395037
	1.4	0.339165	0.338899	0.325793	0.325780	0.319289	0.319289	0.319289
	1.8	0.263793	0.263677	0.251183	0.251177	0.245206	0.245206	0.245206
0.03	0.2	0.497472	0.498327	0.498271	0.498344	0.496405	0.496407	0.496405
	0.6	0.478504	0.479409	0.469157	0.469227	0.461491	0.461492	0.461490
	1.0	0.426619	0.425924	0.409983	0.409908	0.398644	0.398642	0.398642
	1.4	0.355313	0.354062	0.335593	0.335469	0.323131	0.323128	0.323130
	1.8	0.279511	0.279000	0.260334	0.260280	0.248720	0.248719	0.248720
0.05	0.2	0.495475	0.497329	0.498786	0.499002	0.497200	0.497207	0.497198
	0.6	0.482674	0.484728	0.473515	0.473731	0.464020	0.464027	0.464015
	1.0	0.435541	0.434237	0.416929	0.416724	0.402221	0.402214	0.402216
	1.4	0.366525	0.364026	0.343482	0.343135	0.326979	0.326967	0.326976
	1.8	0.290741	0.289779	0.267828	0.267679	0.252260	0.252254	0.252258
0.07	0.2	0.492953	0.496044	0.498803	0.499242	0.497899	0.497918	0.497893
	0.6	0.485425	0.488972	0.477054	0.477506	0.466481	0.466499	0.466468
	1.0	0.442528	0.440625	0.422936	0.422549	0.405771	0.405750	0.405757
	1.4	0.375696	0.371816	0.350478	0.349803	0.330834	0.330800	0.330823
	1.8	0.300116	0.298704	0.274568	0.274285	0.255827	0.255812	0.255822
0.10	0.2	0.488624	0.493945	0.498171	0.499106	0.498766	0.498823	0.498752
	0.6	0.488078	0.494443	0.481373	0.482372	0.470045	0.470099	0.470007
	1.0	0.450999	0.448303	0.430862	0.430121	0.411042	0.410984	0.411001
	1.4	0.387332	0.381265	0.359976	0.358626	0.336627	0.336531	0.336597
	1.8	0.312249	0.310232	0.283856	0.283311	0.261226	0.261183	0.261211

Table 2. MVIM and q-HMTM error comparison of $\mathcal{U}(\psi, \omega)$ for different fractional orders η of Equation (65).

ω	ψ	$ q - HMTM - MVIM _{\eta=0.5}$	$ q - HMTM - MVIM _{\eta=0.7}$	$ q - HMTM - MVIM _{\eta=1.0}$
0.01	0.2	1.30333×10^{-3}	7.25768×10^{-6}	5.57427×10^{-8}
	0.6	7.70615×10^{-3}	6.68658×10^{-6}	4.96941×10^{-8}
	1.0	1.19345×10^{-2}	8.11866×10^{-6}	6.60517×10^{-8}
	1.4	1.33850×10^{-2}	1.29738×10^{-5}	1.03557×10^{-7}
	1.8	1.26157×10^{-2}	5.91413×10^{-6}	4.80566×10^{-8}
0.03	0.2	8.72584×10^{-4}	7.34034×10^{-5}	1.50875×10^{-6}
	0.6	9.27635×10^{-3}	7.07849×10^{-5}	1.36853×10^{-6}
	1.0	1.67114×10^{-2}	7.50900×10^{-5}	1.73553×10^{-6}
	1.4	1.98440×10^{-2}	1.23785×10^{-4}	2.74762×10^{-6}
	1.8	1.92310×10^{-2}	5.48133×10^{-5}	1.26350×10^{-6}

Table 2. Cont.

ω	ψ	$ q - HMTM - MVIM _{\eta=0.5}$	$ q - HMTM - MVIM _{\eta=0.7}$	$ q - HMTM - MVIM _{\eta=1.0}$
0.05	0.2	3.52679×10^{-3}	2.15754×10^{-4}	7.00207×10^{-6}
	0.6	8.94313×10^{-3}	2.15402×10^{-4}	6.45982×10^{-6}
	1.0	1.88162×10^{-2}	2.04378×10^{-4}	7.81329×10^{-6}
	1.4	2.33905×10^{-2}	3.46556×10^{-4}	1.24963×10^{-5}
	1.8	2.30625×10^{-2}	1.49478×10^{-4}	5.69200×10^{-6}
0.07	0.2	6.28892×10^{-3}	4.39441×10^{-4}	1.92607×10^{-5}
	0.6	7.91889×10^{-3}	4.51808×10^{-4}	1.80661×10^{-5}
	1.0	1.99791×10^{-2}	3.87183×10^{-4}	2.08317×10^{-5}
	1.4	2.58931×10^{-2}	6.75072×10^{-4}	3.36748×10^{-5}
	1.8	2.58311×10^{-2}	2.83730×10^{-4}	1.51866×10^{-5}
0.10	0.2	1.04819×10^{-2}	9.35368×10^{-4}	5.63589×10^{-5}
	0.6	5.70595×10^{-3}	9.98903×10^{-4}	5.41592×10^{-5}
	1.0	2.08786×10^{-2}	7.41386×10^{-4}	5.80746×10^{-5}
	1.4	2.87052×10^{-2}	1.34934×10^{-3}	9.54873×10^{-5}
	1.8	2.89380×10^{-2}	5.44985×10^{-4}	4.23852×10^{-5}

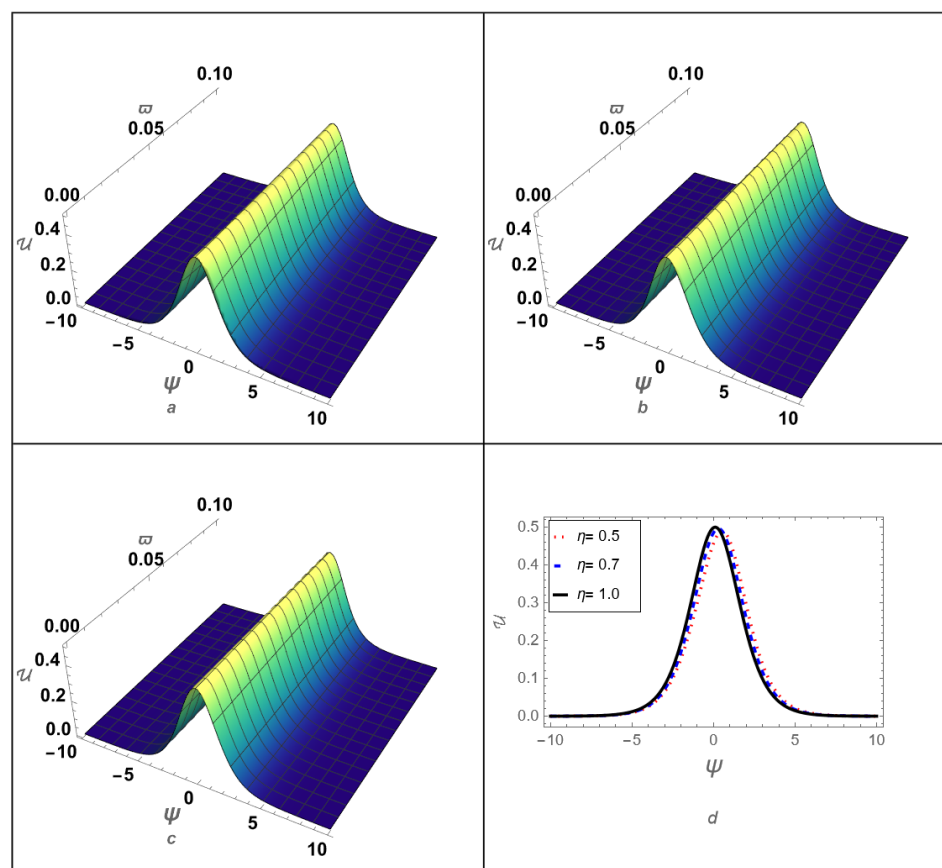


Figure 1. Different fractional-order comparison of the solution $\mathcal{U}(\psi, \omega)$. Part (a) represents the effect of $\eta = 0.5$, part (b) represents the effect of $\eta = 0.7$, part (c) represents the effect of $\eta = 1.0$, and part (d) represents the 2D comparison of the solution $\mathcal{U}(\psi, \omega)$ at $\omega = 0.1$ of Equation (65).

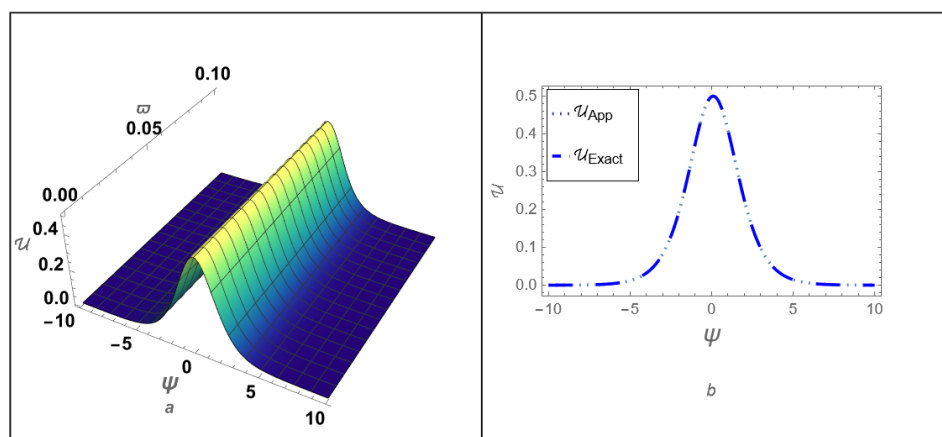


Figure 2. (a) Three-dimensional and (b) two-dimensional representation of the exact and approximate solution $\mathcal{U}(\psi, \omega)$ for $\omega = 0.1$ of Equation (65).

5. Problem 2

5.1. Solution via q -Homotopy Mohand Transform Method

Consider the time fractional-order Rosenau–Hyman equation:

$$D_{\omega}^{\eta} \mathcal{U}(\psi, \omega) - \mathcal{U}(\psi, \omega) \frac{\partial^3 \mathcal{U}(\psi, \omega)}{\partial \psi^3} - 3 \frac{\partial \mathcal{U}(\psi, \omega)}{\partial \psi} \frac{\partial^2 \mathcal{U}(\psi, \omega)}{\partial \psi^2} - \mathcal{U}(\psi, \omega) \frac{\partial \mathcal{U}(\psi, \omega)}{\partial \psi} = 0, \quad (72)$$

where $0 < \eta \leq 1$.

ICs are given as

$$\mathcal{U}(\psi, 0) = -\frac{8c}{3} \cosh^2\left(\frac{\psi}{4}\right), \quad (73)$$

$$\begin{aligned} \mathcal{M}[\mathcal{U}(\psi, \omega)] - s \left(\frac{8c}{3} \cosh^2\left(\frac{\psi}{4}\right) \right) + \frac{1}{s^{\eta}} \mathcal{M} \left[-\mathcal{U}(\psi, \omega) \frac{\partial^3 \mathcal{U}(\psi, \omega)}{\partial \psi^3} - 3 \frac{\partial \mathcal{U}(\psi, \omega)}{\partial \psi} \frac{\partial^2 \mathcal{U}(\psi, \omega)}{\partial \psi^2} \right. \\ \left. - \mathcal{U}(\psi, \omega) \frac{\partial \mathcal{U}(\psi, \omega)}{\partial \psi} \right] = 0. \end{aligned} \quad (74)$$

Non-linear operators are defined as

$$\begin{aligned} \mathcal{N}[\varphi(\psi, \omega; q)] = \mathcal{M}[\varphi(\psi, \omega; q)] - s \left(\frac{8c}{3} \cosh^2\left(\frac{\psi}{4}\right) \right) + \frac{1}{s^{\eta}} \mathcal{M} \left[-\varphi(\psi, \omega; q) \frac{\partial^3 \varphi(\psi, \omega; q)}{\partial \psi^3} - 3 \frac{\partial \varphi(\psi, \omega; q)}{\partial \psi} \times \right. \\ \left. \frac{\partial^2 \varphi(\psi, \omega; q)}{\partial \psi^2} - \varphi(\psi, \omega; q) \frac{\partial \varphi(\psi, \omega; q)}{\partial \psi} \right]. \end{aligned} \quad (75)$$

and the Mohand operators are define as

$$\mathcal{M}[\mathcal{U}_m(\psi, \omega) - k_m \mathcal{U}_{m-1}(\psi, \omega)] = \hbar \mathfrak{h}(\psi, \omega) \mathcal{R}_m[\rightarrow \mathcal{U}_{m-1}]. \quad (76)$$

Here,

$$\begin{aligned} \mathcal{R}_m[\rightarrow \mathcal{U}_{m-1}] = \mathcal{M}[\mathcal{U}_{m-1}(\psi, \omega)] - \left(1 - \frac{k_m}{n} \right) s \left(\frac{8c}{3} \cosh^2\left(\frac{\psi}{4}\right) \right) + \frac{1}{s^{\eta}} \mathcal{M} \left[- \sum_{i=0}^{m-1} \mathcal{U}_i(\psi, \omega) \frac{\partial^3 \mathcal{U}_{m-1-i}(\psi, \omega)}{\partial \psi^3} \right. \\ \left. - 3 \sum_{i=0}^{m-1} \frac{\partial \mathcal{U}_i(\psi, \omega)}{\partial \psi} \frac{\partial^2 \mathcal{U}_{m-1-i}(\psi, \omega)}{\partial \psi^2} - \sum_{i=0}^{m-1} \mathcal{U}_i(\psi, \omega) \frac{\partial \mathcal{U}_{m-1-i}(\psi, \omega)}{\partial \psi} \right], \end{aligned} \quad (77)$$

$$\mathcal{U}_m(\psi, \omega) = k_m \mathcal{U}_{m-1}(\psi, \omega) + \hbar \mathcal{M}^{-1}[\mathfrak{h}(\psi, \omega) \mathcal{R}_m(\rightarrow \mathcal{U}_{m-1})]. \quad (78)$$

Based on the initial constraint of Equation (78), the subsequent result is obtained:

$$\begin{aligned}\mathcal{U}_1(\psi, \omega) &= -\frac{2c^2\hbar\left(5\sinh\left(\frac{\psi}{2}\right) + 4\sinh(\psi)\right)\omega^\eta}{9\Gamma(\eta+1)}, \\ \mathcal{U}_2(\psi, \omega) &= \frac{1}{27}c^2\hbar\omega^\eta\left(-\frac{c\hbar\left(35\cosh\left(\frac{\psi}{2}\right) + 78\cosh\left(\frac{3\psi}{2}\right) + 104\cosh(\psi)\right)\omega^\eta}{\Gamma(2\eta+1)}\right. \\ &\quad \left.-\frac{6\left(5\sinh\left(\frac{\psi}{2}\right) + 4\sinh(\psi)\right)(n+\hbar)}{\Gamma(\eta+1)}\right)\end{aligned}\quad (79)$$

and so on.

In the same way, the remaining components are acquired. The q-HMTM solution of Equation (72) is subsequently derived.

$$\mathcal{U}(\psi, \omega) = \mathcal{U}_0 + \sum_{m=1}^{\infty} \mathcal{U}_m \left(\frac{1}{n}\right)^m. \quad (80)$$

$$\begin{aligned}\mathcal{U}(\psi, \omega) &= -\frac{8c}{3}\cosh^2\left(\frac{\psi}{4}\right) - \frac{2c^2\hbar\left(5\sinh\left(\frac{\psi}{2}\right) + 4\sinh(\psi)\right)\omega^\eta}{9\Gamma(\eta+1)} - \frac{1}{27}c^2\hbar\omega^\eta\left(-\frac{6\left(5\sinh\left(\frac{\psi}{2}\right) + 4\sinh(\psi)\right)(n+\hbar)}{\Gamma(\eta+1)}\right. \\ &\quad \left.-\frac{c\hbar\left(35\cosh\left(\frac{\psi}{2}\right) + 78\cosh\left(\frac{3\psi}{2}\right) + 104\cosh(\psi)\right)\omega^\eta}{\Gamma(2\eta+1)}\right) + \dots.\end{aligned}\quad (81)$$

The approximate solution $\sum_{m=1}^N \mathcal{U}_m \left(\frac{1}{n}\right)^m$ for the values $\eta = 1$, $\hbar = -1$ and $n = 1$ converges to the exact solution as $N \rightarrow \infty$.

$$\mathcal{U}(\psi, \omega) = -\frac{8c}{3}\cosh^2\left(\frac{1}{4}(\psi - c\omega)\right). \quad (82)$$

5.2. Solution via Mohand Variational Iteration Transform Method

Consider the time fractional-order Rosenau–Hyman equation:

$$D_\omega^\eta \mathcal{U}(\psi, \omega) = \mathcal{U}(\psi, \omega) \frac{\partial^3 \mathcal{U}(\psi, \omega)}{\partial \psi^3} + 3 \frac{\partial \mathcal{U}(\psi, \omega)}{\partial \psi} \frac{\partial^2 \mathcal{U}(\psi, \omega)}{\partial \psi^2} + \mathcal{U}(\psi, \omega) \frac{\partial \mathcal{U}(\psi, \omega)}{\partial \psi}, \quad (83)$$

where $0 < \eta \leq 1$.

ICs are given as

$$\mathcal{U}(\psi, 0) = -\frac{8c}{3}\cosh^2\left(\frac{\psi}{4}\right), \quad (84)$$

The following result is obtained by employing the iterative scheme (83):

$$\begin{aligned}\mathcal{U}_{n+1}(\psi, \omega) &= \mathcal{U}_n(\psi, \omega) + \mathcal{M}^{-1} \left[\frac{1}{s^\eta} \sum_{k=0}^{m-1} s^{\eta-k-1} \frac{\partial^k \mathcal{U}(\psi, 0)}{\partial \omega^k} + \mathcal{M}[\mathcal{U}_n(\psi, \omega) \frac{\partial^3 \mathcal{U}_n(\psi, \omega)}{\partial \psi^3} + 3 \frac{\partial \mathcal{U}_n(\psi, \omega)}{\partial \psi} \frac{\partial^2 \mathcal{U}_n(\psi, \omega)}{\partial \psi^2} \right. \\ &\quad \left. + \mathcal{U}_n(\psi, \omega) \frac{\partial \mathcal{U}_n(\psi, \omega)}{\partial \psi} \right],\end{aligned}\quad (85)$$

To obtain the second approximate solution, put $n = 0$.

$$\begin{aligned}\mathcal{U}_1(\psi, \omega) &= \mathcal{U}_0(\psi, \omega) + \mathcal{M}^{-1} \left[\frac{1}{s^\eta} \sum_{k=0}^{m-1} s^{\eta-k-1} \frac{\partial^k \mathcal{U}(\psi, 0)}{\partial \omega^k} + \mathcal{M}[\mathcal{U}_0(\psi, \omega) \frac{\partial^3 \mathcal{U}_0(\psi, \omega)}{\partial \psi^3} + 3 \frac{\partial \mathcal{U}_0(\psi, \omega)}{\partial \psi} \frac{\partial^2 \mathcal{U}_0(\psi, \omega)}{\partial \psi^2} \right. \\ &\quad \left. + \mathcal{U}_0(\psi, \omega) \frac{\partial \mathcal{U}_0(\psi, \omega)}{\partial \psi} \right],\end{aligned}\quad (86)$$

The subsequent result is obtained by simplifying the previous result:

$$\mathcal{U}_1(\psi, \omega) = -\frac{8c}{3} \cosh^2\left(\frac{\psi}{4}\right) + \frac{2c^2 \left(5 \sinh\left(\frac{\psi}{2}\right) + 4 \sinh(\psi)\right) \omega^\eta}{9\Gamma(\eta + 1)}. \quad (87)$$

Insert $n = 1$ to obtain the following result:

$$\begin{aligned} \mathcal{U}_2(\psi, \omega) = \mathcal{U}_1(\psi, \omega) + \mathcal{M}^{-1} \left[\frac{1}{s^\eta} \sum_{k=0}^{m-1} s^{\eta-k-1} \frac{\partial^k \mathcal{U}(\psi, 0)}{\partial \omega^k} + \mathcal{M}[\mathcal{U}_1(\psi, \omega) \frac{\partial^3 \mathcal{U}_1(\psi, \omega)}{\partial \psi^3} + 3 \frac{\partial \mathcal{U}_1(\psi, \omega)}{\partial \psi} \frac{\partial^2 \mathcal{U}_1(\psi, \omega)}{\partial \psi^2} \right. \\ \left. + \mathcal{U}_1(\psi, \omega) \frac{\partial \mathcal{U}_1(\psi, \omega)}{\partial \psi} \right], \end{aligned} \quad (88)$$

The final approximate solution that emerges from the simplification is as follows:

$$\begin{aligned} \mathcal{U}_2(\psi, \omega) = \frac{1}{3}(-8)c \cosh^2\left(\frac{\psi}{4}\right) + \frac{2c^2 \left(5 \sinh\left(\frac{\psi}{2}\right) + 4 \sinh(\psi)\right) \omega^\eta}{9\Gamma(\eta + 1)} \\ - \frac{c^3 \left(35 \cosh\left(\frac{\psi}{2}\right) + 78 \cosh\left(\frac{3\psi}{2}\right) + 104 \cosh(\psi)\right) \omega^{2\eta}}{27\Gamma(2\eta + 1)} \\ + \frac{5c^4 \left(-5 \sinh\left(\frac{\psi}{2}\right) + 39 \sinh\left(\frac{3\psi}{2}\right) + 10 \sinh(\psi) + 32 \sinh(2\psi)\right) \omega^{3\eta} \Gamma(2\eta + 1)}{81\Gamma(\eta + 1)^2 \Gamma(3\eta + 1)}. \end{aligned} \quad (89)$$

The time fractional-order Rosenau–Hyman equation is analyzed in detail using both the MVIM and q-HMTM methodologies. The results are presented through comprehensive comparisons and visualizations. Table 3 provides a comparison of the solutions $\mathcal{U}(\psi, \omega)$ obtained using MVIM and q-HMTM for different fractional orders η of Equation (72). The table highlights the consistency and accuracy of the two methods across varying η values, demonstrating their robustness in solving fractional-order models. Figure 3 illustrates the effect of different fractional orders η on the solution $\mathcal{U}(\psi, \omega)$: Figure 3a: Depicts the solution behavior for $\eta = 0.5$, showing a more diffusive wave pattern. Figure 3b: Represents the solution for $\eta = 0.7$, illustrating a transition to more defined wave structures. Figure 3c: Highlights the solution for $\eta = 1.0$, corresponding to the integer-order case, with the wave profiles becoming sharper and more structured. Figure 3d: Shows a 2D comparison of the solution $\mathcal{U}(\psi, \omega)$ at $\omega = 0.1$, offering a detailed perspective on the impact of the fractional order on the solutions evolution. Figure 4 provides both 3D and 2D visualizations of the exact and approximate solutions $\mathcal{U}(\psi, \omega)$ for $\omega = 0.1$ of Equation (72). The graphical representations underscore the high degree of agreement between the methods, showcasing their precision and reliability in modeling the dynamic behavior of the fractional system. Table 4 presents an error analysis, comparing the solutions $\mathcal{U}(\psi, \omega)$ derived using MVIM and q-HMTM for various fractional orders η of Equation (72). The error values demonstrate the excellent accuracy of both methods, further validating their applicability to fractional differential equations.

Table 3. MVIM and q-HMTM solution comparison of $\mathcal{U}(\psi, \omega)$ for different fractional orders η of Equation (72).

ω	ψ	q-HMTM	MVIM	q-HMTM	MVIM	q-HMTM	MVIM	<i>Exact</i>
		$\eta = 0.5$	$\eta = 0.5$	$\eta = 0.7$	$\eta = 0.7$	$\eta = 1.0$	$\eta = 1.0$	
0.01	0.2	−0.267089	−0.267089	−0.267217	−0.267217	−0.267305	−0.267305	−0.267327
	0.6	−0.271792	−0.271792	−0.272328	−0.272328	−0.272622	−0.272622	−0.272692
	1.0	−0.281993	−0.281992	−0.282990	−0.282990	−0.283522	−0.283522	−0.283649
	1.4	−0.298047	−0.298044	−0.299606	−0.299606	−0.300437	−0.300437	−0.300639
	1.8	−0.320528	−0.320522	−0.322811	−0.322811	−0.324038	−0.324038	−0.324343
0.03	0.2	−0.267014	−0.267013	−0.267109	−0.267108	−0.267251	−0.267251	−0.267314
	0.6	−0.271246	−0.271243	−0.271917	−0.271916	−0.272445	−0.272445	−0.272651
	1.0	−0.280936	−0.280930	−0.282233	−0.282232	−0.283203	−0.283203	−0.283579
	1.4	−0.296390	−0.296377	−0.298422	−0.298421	−0.299938	−0.299938	−0.300538
	1.8	−0.318134	−0.318106	−0.321071	−0.321069	−0.323301	−0.323301	−0.324206
0.05	0.2	−0.267014	−0.267012	−0.267042	−0.267042	−0.267199	−0.267199	−0.267301
	0.6	−0.270933	−0.270927	−0.271612	−0.271611	−0.272272	−0.272272	−0.272611
	1.0	−0.280297	−0.280283	−0.281661	−0.281660	−0.282889	−0.282889	−0.283510
	1.4	−0.295386	−0.295357	−0.297528	−0.297524	−0.299449	−0.299449	−0.300437
	1.8	−0.316706	−0.316647	−0.319765	−0.319758	−0.322578	−0.322578	−0.324070
0.07	0.2	−0.267045	−0.267042	−0.266998	−0.266997	−0.267151	−0.267151	−0.267288
	0.6	−0.270716	−0.270706	−0.271361	−0.271359	−0.272103	−0.272103	−0.272571
	1.0	−0.279830	−0.279808	−0.281182	−0.281179	−0.282582	−0.282582	−0.283441
	1.4	−0.294651	−0.294604	−0.296777	−0.296770	−0.298968	−0.298968	−0.300336
	1.8	−0.315678	−0.315580	−0.318675	−0.318661	−0.321869	−0.321869	−0.323934
0.10	0.2	−0.267123	−0.267118	−0.266961	−0.266960	−0.267085	−0.267085	−0.267269
	0.6	−0.270491	−0.270474	−0.271049	−0.271045	−0.271858	−0.271858	−0.272511
	1.0	−0.279310	−0.279271	−0.280573	−0.280566	−0.282131	−0.282130	−0.283338
	1.4	−0.293830	−0.293749	−0.295823	−0.295808	−0.298263	−0.298262	−0.300186
	1.8	−0.314551	−0.314384	−0.317299	−0.317269	−0.320833	−0.320831	−0.323730

Table 4. MVIM and q-HMTM error comparison of $\mathcal{U}(\psi, \omega)$ for different fractional orders η of Equation (72).

ω	ψ	$ q - HMTM - MVIM _{\eta=0.5}$	$ q - HMTM - MVIM _{\eta=0.7}$	$ q - HMTM - MVIM _{\eta=1.0}$
0.01	0.2	1.28355×10^{-4}	7.07481×10^{-9}	5.45943×10^{-11}
	0.6	5.36366×10^{-4}	2.48460×10^{-8}	1.91730×10^{-10}
	1.0	9.96743×10^{-4}	5.55279×10^{-8}	4.28493×10^{-10}
	1.4	1.55913×10^{-3}	1.15788×10^{-7}	8.93505×10^{-10}
	1.8	2.28322×10^{-3}	2.39517×10^{-7}	1.84828×10^{-9}
0.03	0.2	9.42819×10^{-5}	7.10673×10^{-8}	1.47404×10^{-9}
	0.6	6.70136×10^{-4}	2.49581×10^{-7}	5.17671×10^{-9}
	1.0	1.29608×10^{-3}	5.57784×10^{-7}	1.15693×10^{-8}
	1.4	2.03085×10^{-3}	1.16310×10^{-6}	2.41246×10^{-8}
	1.8	2.93532×10^{-3}	2.40597×10^{-6}	4.99037×10^{-8}
0.05	0.2	2.74311×10^{-5}	2.07755×10^{-7}	6.82430×10^{-9}
	0.6	6.77663×10^{-4}	7.29615×10^{-7}	2.39662×10^{-8}
	1.0	1.36269×10^{-4}	1.63060×10^{-6}	5.35617×10^{-8}
	1.4	2.13836×10^{-4}	3.40017×10^{-6}	1.11688×10^{-7}
	1.8	3.05185×10^{-4}	7.03353×10^{-6}	2.31036×10^{-7}

Table 4. Cont.

ω	ψ	$ q - HMTM - MVIM _{\eta=0.5}$	$ q - HMTM - MVIM _{\eta=0.7}$	$ q - HMTM - MVIM _{\eta=1.0}$
0.07	0.2	4.75401×10^{-5}	4.21134×10^{-7}	1.87258×10^{-8}
	0.6	6.42608×10^{-4}	1.47898×10^{-6}	6.57634×10^{-8}
	1.0	1.34846×10^{-3}	3.30534×10^{-6}	1.46973×10^{-7}
	1.4	2.11898×10^{-3}	6.89239×10^{-6}	3.06472×10^{-7}
	1.8	2.98302×10^{-3}	1.42575×10^{-5}	6.33962×10^{-7}
0.10	0.2	1.63260×10^{-4}	8.90666×10^{-7}	5.45944×10^{-8}
	0.6	5.54189×10^{-4}	3.12793×10^{-6}	1.91730×10^{-7}
	1.0	1.25622×10^{-3}	6.99055×10^{-6}	4.28493×10^{-7}
	1.4	1.97811×10^{-3}	1.45769×10^{-5}	8.93505×10^{-7}
	1.8	2.71761×10^{-3}	3.01534×10^{-5}	1.84828×10^{-6}

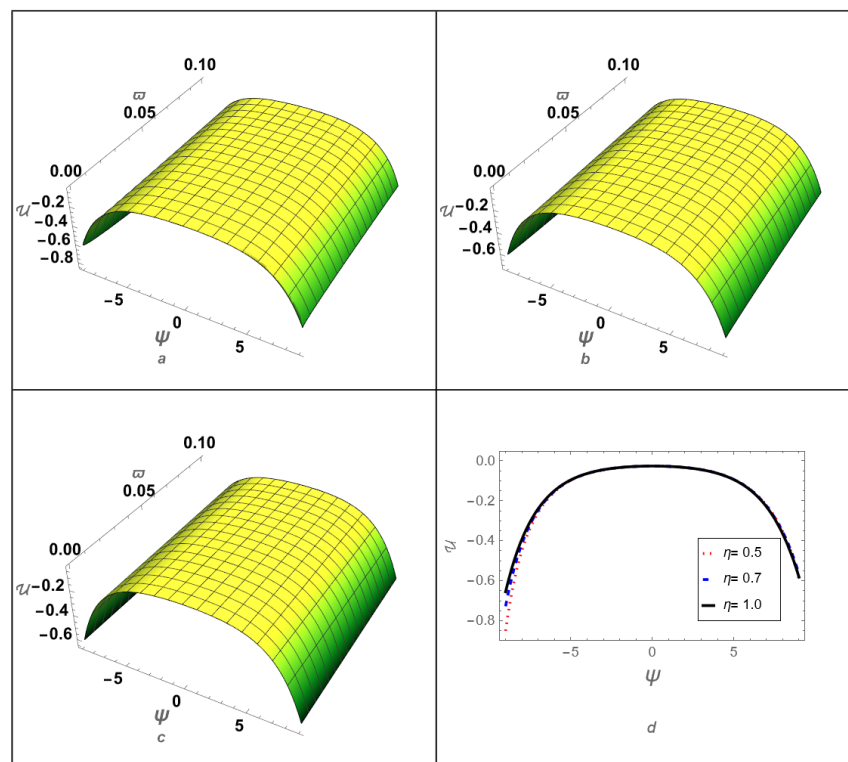


Figure 3. Different fractional-order comparison of the solution $\mathcal{U}(\psi, \omega)$. Part (a) represents the effect of $\eta = 0.5$, part (b) represents the effect of $\eta = 0.7$, part (c) represents the effect of $\eta = 1.0$, and part (d) represents the 2D comparison of the solution $\mathcal{U}(\psi, \omega)$ at $\omega = 0.1$ of Equation (72).

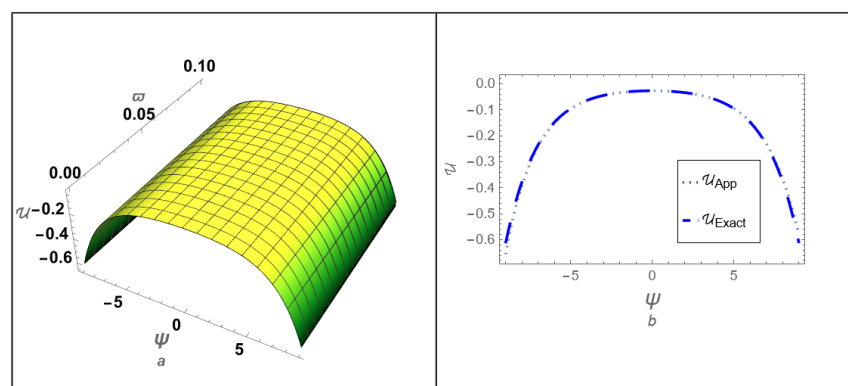


Figure 4. (a) Three-dimensional and (b) two-dimensional representation of the exact and approximate solution $\mathcal{U}(\psi, \omega)$ for $\omega = 0.1$ of Equation (72).

6. Conclusions

In this work, we explored fractional-order Sawada–Kotera and Rosenau–Hyman equations using two advanced analytical techniques: the q-homotopy Mohand transform method (q-HMTM) and the Mohand variational iteration method (MVIM). These methodologies, combined with the Caputo fractional operator, provided a powerful framework for solving complex non-linear fractional differential equations. We successfully derived hyperbolic, trigonometric, and rational solutions, demonstrating the adaptability of the proposed methods to various solution forms. The results reveal the significant influence of the fractional parameter on the behavior of solutions, providing a deeper understanding of diffusion and wave dynamics in fractional-order systems. Graphical visualizations supported the theoretical findings, illustrating the practical relevance of the derived solutions in explaining physical phenomena. This study highlights the effectiveness and reliability of q-HMTM and MVIM as robust tools for analyzing fractional-order equations. These methods not only simplify the solution process but also provide new insights into the dynamics of fractional systems, offering applications across diverse fields, including fluid mechanics, wave propagation, and non-linear dynamics. Future research may extend the proposed approaches to more complex fractional models and explore their potential in multidisciplinary applications.

Author Contributions: Conceptualization, K.A.R. and M.Y.A.; methodology, H.A.; software, T.S.A.; validation, A.A.; formal analysis, K.A.R.; investigation, M.Y.A.; resources, H.A.; data curation, A.A.; writing—original draft preparation, K.A.R.; writing—review and editing, M.Y.A.; visualization, H.A.; supervision, A.A.; project administration, T.S.A.; funding acquisition, M.Y.A. All authors have read and agreed to the published version of the manuscript.

Funding: This research was funded by the Deanship of Graduate Studies and Scientific Research, Jazan University, Saudi Arabia, through project number RG24-L02.

Data Availability Statement: The original contributions presented in this study are included in this article; further inquiries can be directed to the corresponding author.

Acknowledgments: The authors gratefully acknowledge the funding of the Deanship of Graduate Studies and Scientific Research, Jazan University, Saudi Arabia, through project number RG24-L02.

Conflicts of Interest: The authors declare no conflicts of interest.

References

- Guo, T.; Nikan, O.; Avazzadeh, Z.; Qiu, W. Efficient alternating direction implicit numerical approaches for multi-dimensional distributed-order fractional integro differential problems. *Comput. Appl. Math.* **2022**, *41*, 236. [\[CrossRef\]](#)
- Tansri, K.; Kittisopaporn, A.; Chansangiam, P. Numerical solutions of the space-time fractional diffusion equation via a gradient-descent iterative procedure. *J. Math. Comput. Sci.* **2023**, *31*, 353–366. [\[CrossRef\]](#)
- Zhang, R.F.; Bilige, S. Bilinear neural network method to obtain the exact analytical solutions of nonlinear partial differential equations and its application to p-gBKP equation. *Nonlinear Dyn.* **2019**, *95*, 3041–3048. [\[CrossRef\]](#)
- Zhang, R.F.; Li, M.C. Bilinear residual network method for solving the exactly explicit solutions of nonlinear evolution equations. *Nonlinear Dyn.* **2022**, *108*, 521–531. [\[CrossRef\]](#)
- Alam, N.; Ullah, M.S.; Nofal, T.A.; Ahmed, H.M.; Ahmed, K.K.; AL-Nahhas, M.A. Novel dynamics of the fractional KFG equation through the unified and unified solver schemes with stability and multistability analysis. *Nonlinear Eng.* **2024**, *13*, 20240034. [\[CrossRef\]](#)
- Alam, N.; Akbar, A.; Ullah, M.S.; Mostafa, M. Dynamic waveforms of the new Hamiltonian amplitude model using three different analytic techniques. *Indian J. Phys.* **2024**. [\[CrossRef\]](#)
- Ganie, A.H.; AlBaidani, M.M.; Wazwaz, A.M.; Ma, W.X.; Shamima, U.; Ullah, M.S. Soliton dynamics and chaotic analysis of the Biswas-Arshed model. *Opt. Quantum Electron.* **2024**, *56*, 1379. [\[CrossRef\]](#)
- Singh, J.; Kumar, D.; Kilicman, A. Numerical solutions of nonlinear fractional partial differential equations arising in spatial diffusion of biological populations. In *Abstract and Applied Analysis*; Hindawi Publishing Corporation: Cairo, Egypt, 2014; Volume 2014, p. 535793.

9. Stevik, T.K.; Aa, K.; Ausl, G.; Hanssen, J.F. Retention and removal of pathogenic bacteria in wastewater percolating through porous media: A review. *Water Res.* **2004**, *38*, 1355–1367. [CrossRef] [PubMed]
10. Khan, M.A.; Ullah, S.; Farooq, M. A new fractional model for tuberculosis with relapse via Atangana-Baleanu derivative. *Chaos Solitons Fractals* **2018**, *116*, 227–238. [CrossRef]
11. Shivanian, E.; Jafarabadi, A. Time fractional modified anomalous sub-diffusion equation with a nonlinear source term through locally applied meshless radial point interpolation. *Mod. Phys. Lett. B* **2018**, *32*, 1850251. [CrossRef]
12. Vinagre, B.M.; Feliu, V. Modeling and control of dynamic system using fractional calculus: Application to electrochemical processes and flexible structures. In Proceedings of the 41st IEEE Conference on Decision and Control, Las Vegas, NV, USA, 10–13 December 2002; Volume 1, pp. 214–239.
13. Chen, Y.; Petras, I.; Xue, D. Fractional order control-a tutorial. In Proceedings of the 2009 American Control Conference, St. Louis, MO, USA, 10–12 June 2009; IEEE: Piscataway, NJ, USA, 2009; pp. 1397–1411.
14. Singh, J.; Kumar, D.; Baleanu, D.; Rathore, S. An efficient numerical algorithm for the fractional Drinfeld-Sokolov-Wilson equation. *Appl. Math. Comput.* **2018**, *335*, 12–24. [CrossRef]
15. Kumar, D.; Tchier, F.; Singh, J.; Baleanu, D. An efficient computational technique for fractal vehicular traffic flow. *Entropy* **2018**, *20*, 259. [CrossRef] [PubMed]
16. Safari, M.; Ganji, D.D.; Moslemi, M. Application of He’s variational iteration method and Adomian’s decomposition method to the fractional KdV-Burgers-Kuramoto equation. *Comput. Math. Appl.* **2009**, *58*, 2091–2097. [CrossRef]
17. Prakash, A. Analytical method for space-fractional telegraph equation by homotopy perturbation transform method. *Nonlinear Eng.* **2016**, *5*, 123–128. [CrossRef]
18. Jain, S. Numerical analysis for the fractional diffusion and fractional Buckmaster equation by the two-step Laplace Adam-Bashforth method. *Eur. Phys. J. Plus* **2018**, *133*, 19. [CrossRef]
19. Yin, C.; Huang, X.; Dadras, S.; Cheng, Y.; Cao, J.; Malek, H.; Mei, J. Design of optimal lighting control strategy based on multi-variable fractional-order extremum seeking method. *Inf. Sci.* **2018**, *465*, 38–60. [CrossRef]
20. He, Y.; Kai, Y. Wave structures, modulation instability analysis and chaotic behaviors to Kudryashov’s equation with third-order dispersion. *Nonlinear Dyn.* **2024**, *112*, 10355–10371. [CrossRef]
21. Xie, J.; Xie, Z.; Xu, H.; Li, Z.; Shi, W.; Ren, J.; Shi, H. Resonance and attraction domain analysis of asymmetric duffing systems with fractional damping in two degrees of freedom. *Chaos Solitons Fractals* **2024**, *187*, 115440. [CrossRef]
22. Feng, G.; Yu, S.; Wang, D.; Zhang, Z. Discussion on the Weak Equivalence Principle for a Schwarzschild Gravitational Field based on the Light-Clock Model. *Ann. Phys.* **2024**, *473*, 169903. <https://doi.org/10.1016/j.aop.2024.169903>. [CrossRef]
23. Jin, Y.; Lu, G.; Sun, W. Genuine multipartite entanglement from a thermodynamic perspective. *Phys. Rev. A* **2024**, *109*, 042422. [CrossRef]
24. Shuangjian, G.; Apurba, D. Cohomology and deformations of generalised reynolds operators on leibni algebras. *Rocky Mt. J. Math.* **2024**, *54*, 161–178. [CrossRef]
25. Yasmin, H.; Alshehry, A.S.; Ganie, A.H.; Mahnashi, A.M. Perturbed Gerdjikov-Ivanov equation: Soliton solutions via Backlund transformation. *Optik* **2024**, *298*, 171576. [CrossRef]
26. Alderremy, A.A.; Iqbal, N.; Aly, S.; Nonlaopon, K. Fractional series solution construction for nonlinear fractional reaction-diffusion Brusselator model utilizing Laplace residual power series. *Symmetry* **2022**, *14*, 1944. [CrossRef]
27. Al-Sawalha, M.M.; Khan, A.; Ababneh, O.Y.; Botmart, T. Fractional view analysis of Kersten-Krasil’shchik coupled KdV-mKdV systems with non-singular kernel derivatives. *AIMS Math* **2022**, *7*, 18334–18359. [CrossRef]
28. Naeem, M.; Rezazadeh, H.; Khammash, A.A.; Shah, R.; Zal, S. Analysis of the Fuzzy Fractional-Order Solitary Wave Solutions for the KdV Equation in the Sense of Caputo-Fabrizio Derivative. *J. Math.* **2022**, *2022*, 3688916. [CrossRef]
29. Alqhtani, M.; Saad, K.M.; Shah, R.; Hamanah, W.M. Discovering novel soliton solutions for (3+1)-modified fractional Zakharov-Kuznetsov equation in electrical engineering through an analytical approach. *Opt. Quantum Electron.* **2023**, *55*, 1149. [CrossRef]
30. Alqhtani, M.; Saad, K.M.; Shah, R.; Weera, W.; Hamanah, W.M. Analysis of the fractional-order local Poisson equation in fractal porous media. *Symmetry* **2022**, *14*, 1323. [CrossRef]
31. Zheng, B.; Wen, C. Exact solutions for fractional partial differential equations by a new fractional sub-equation method. *Adv. Differ. Equations* **2013**, *2013*, 199. [CrossRef]
32. Naher, H.; Abdullah, F.A.; Mohyud-Din, S.T. Extended generalized Riccati equation mapping method for the fifth-order Sawada-Kotera equation. *Aip Adv.* **2013**, *3*, 052104. [CrossRef]
33. Dinarv, S.; Khosravi, S.; Doosthoseini, A.; Rashidi, M.M. The homotopy analysis method for solving the Sawada-Kotera and Lax’s fifth-order KdV equations. *Adv. Theor. Appl. Mech.* **2008**, *1*, 327–335.
34. Wazwaz, A.M. *Partial Differential Equations and Solitary Waves Theory*; Springer Science and Business Media: Berlin/Heidelberg, Germany, 2010.
35. Debnath, L.; Debnath, L. *Nonlinear Partial Differential Equations for Scientists and Engineers*; Birkhauser: Boston, MA, USA, 2005; pp. 528–529.

36. Rosenau, P.; Hyman, J.M. Compactons: Solitons with finite wavelength. *Phys. Rev. Lett.* **1993**, *70*, 564. [[CrossRef](#)] [[PubMed](#)]
37. Mihaila, B.; Cardenas, A.; Cooper, F.; Saxena, A. Stability and dynamical properties of Rosenau-Hyman compactons using Pade approximants. *Phys. Rev. E-Stat. Nonlinear Soft Matter Phys.* **2010**, *81*, 056708. [[CrossRef](#)] [[PubMed](#)]
38. Rus, F.; Villatoro, F.R. Self-similar radiation from numerical Rosenau-Hyman compactons. *J. Comput. Phys.* **2007**, *227*, 440–454. [[CrossRef](#)]
39. Rus, F.; Villatoro, F.R. Numerical methods based on modified equations for nonlinear evolution equations with compactons. *Appl. Math. Comput.* **2008**, *204*, 416–422. [[CrossRef](#)]
40. Iyiola, O.S.; Ojo, G.O.; Mmaduabuchi, O. The fractional Rosenau-Hyman model and its approximate solution. *Alex. Eng. J.* **2016**, *55*, 1655–1659. [[CrossRef](#)]
41. Singh, J.; Kumar, D.; Swroop, R.; Kumar, S. An efficient computational approach for time-fractional Rosenau-Hyman equation. *Neural Comput. Appl.* **2018**, *30*, 3063–3070. [[CrossRef](#)]
42. Yulita, Molliq, R.; Noorani, M.S.M. Solving the Fractional Rosenau-Hyman Equation via Variational Iteration Method and Homotopy Perturbation Method. *Int. J. Differ. Equations* **2012**, *2012*, 472030.
43. Senol, M.; Tasbozan, O.; Kurt, A. Comparison of two reliable methods to solve fractional Rosenau-Hyman equation. *Math. Methods Appl. Sci.* **2021**, *44*, 7904–7914. [[CrossRef](#)]
44. Cinar, M.; Secer, A.; Bayram, M. An application of Genocchi wavelets for solving the fractional Rosenau-Hyman equation? *Alex. Eng. J.* **2021**, *60*, 5331–5340. [[CrossRef](#)]
45. Ajibola, S.O.; Oke, A.S.; Mutuku, W.N. LHAM approach to fractional order Rosenau-Hyman and Burgers' equations. *Asian Res. J. Math.* **2020**, *16*, 1–14. [[CrossRef](#)]
46. He, J.H. Some asymptotic methods for strongly nonlinear equations. *Int. J. Mod. Phys.* **2006**, *20*, 1141–1199. [[CrossRef](#)]
47. He, J.H. *Non-Perturbative Methods for Strongly Nonlinear Problems*; de-Verlag im Internet GmbH: Berlin, Germany, 2006.
48. He, J.H. Variational iteration method some recent results and new interpretations. *J. Comput. Appl. Math.* **2007**, *207*, 3–17. [[CrossRef](#)]
49. He, J.H. Variational iteration method a kind of non-linear analytical technique: Some examples. *Int. J. Non-Linear Mech.* **1999**, *34*, 699–708. [[CrossRef](#)]
50. He, J.H.; Wu, X.H. Construction of solitary solution and compacton-like solution by variational iteration method. *Chaos Solitons Fractals* **2006**, *29*, 108–113. [[CrossRef](#)]
51. He, J.H. Addendum: New interpretation of homotopy perturbation method. *Int. J. Mod. Phys.* **2006**, *20*, 2561–2568. [[CrossRef](#)]
52. He, J.H. Variational principles for some nonlinear partial differential equations with variable coefficients. *Chaos Solitons Fractals* **2004**, *19*, 847–851. [[CrossRef](#)]
53. Marinca, V. An approximate solution for one-dimensional weakly nonlinear oscillations. *Int. J. Nonlinear Sci. Numer. Simul.* **2002**, *3*, 107–120. [[CrossRef](#)]
54. Abdou, M.A.; Soliman, A.A. New applications of variational iteration method. *Phys. Nonlinear Phenom.* **2005**, *211*, 1–8. [[CrossRef](#)]
55. Abdou, M.A.; Soliman, A.A. Variational iteration method for solving Burger's and coupled Burger's equations. *J. Comput. Appl. Math.* **2005**, *181*, 245–251. [[CrossRef](#)]
56. Abulwafa, E.M.; Abdou, M.A.; Mahmoud, A.A. The solution of nonlinear coagulation problem with mass loss. *Chaos Solitons Fractals* **2006**, *29*, 313–330. [[CrossRef](#)]
57. Abulwafa, E.M.; Abdou, M.A.; Mahmoud, A.A. Nonlinear fluid flows in pipe-like domain problem using variational-iteration method. *Chaos Solitons Fractals* **2007**, *32*, 1384–1397. [[CrossRef](#)]
58. Soliman, A.A.; Abdou, M.A. Numerical solutions of nonlinear evolution equations using variational iteration method. *J. Comput. Appl. Math.* **2007**, *207*, 111–120. [[CrossRef](#)]
59. Bildik, N.; Konuralp, A. The use of variational iteration method, differential transform method and Adomian decomposition method for solving different types of nonlinear partial differential equations. *Int. J. Nonlinear Sci. Numer. Simul.* **2006**, *7*, 65–70. [[CrossRef](#)]
60. Abdou, M.A. On the variational iteration method. *Phys. Lett. A* **2007**, *366*, 61–68. [[CrossRef](#)]
61. Sweilam, N.H.; Khader, M.M. Variational iteration method for one dimensional nonlinear thermoelasticity. *Chaos Solitons Fractals* **2007**, *32*, 145–149. [[CrossRef](#)]
62. Momani, S.; Odibat, Z. Numerical comparison of methods for solving linear differential equations of fractional order. *Chaos Solitons Fractals* **2007**, *31*, 1248–1255. [[CrossRef](#)]
63. Kaya, D. An explicit and numerical solutions of some fifth-order KdV equation by decomposition method. *Appl. Math. Comput.* **2003**, *144*, 353–363. [[CrossRef](#)]
64. Liao, S. On the homotopy analysis method for nonlinear problems. *Appl. Math. Comput.* **2004**, *147*, 499–513. [[CrossRef](#)]
65. Prakash, A.; Kaur, H. Numerical solution for fractional model of Fokker-Planck equation by using q-HATM. *Chaos Solitons Fractals* **2017**, *105*, 99–110. [[CrossRef](#)]

66. Srivastava, H.M.; Kumar, D.; Singh, J. An efficient analytical technique for fractional model of vibration equation. *Appl. Math. Model.* **2017**, *45*, 192–204. [[CrossRef](#)]
67. Kumar, D.; Singh, J.; Baleanu, D. A new numerical algorithm for fractional Fitzhugh-Nagumo equation arising in transmission of nerve impulses. *Nonlinear Dyn.* **2018**, *91*, 307–317. [[CrossRef](#)]
68. Singh, J.; Kumar, D.; Swroop, R. Numerical solution of time-and space-fractional coupled Burgers' equations via homotopy algorithm. *Alex. Eng. J.* **2016**, *55*, 1753–1763. [[CrossRef](#)]
69. Moh, M.; Mahgoub, A. The new integral transform "Mohand Transform". *Adv. Theor. Appl. Math.* **2017**, *12*, 113–120.
70. Nadeem, M.; He, J.H.; Islam, A. The homotopy perturbation method for fractional differential equations: Part 1 Mohand transform. *Int. J. Numer. Heat Fluid Flow* **2021**, *31*, 3490–3504. [[CrossRef](#)]

Disclaimer/Publisher's Note: The statements, opinions and data contained in all publications are solely those of the individual author(s) and contributor(s) and not of MDPI and/or the editor(s). MDPI and/or the editor(s) disclaim responsibility for any injury to people or property resulting from any ideas, methods, instructions or products referred to in the content.